Journal of Pathology
J Pathol December 2021; **255:** 374–386
Published online 6 September 2021 in Wiley Online Library (wileyonlinelibrary.com) DOI: 10.1002/path.5776

ORIGINAL PAPER

Calcyphosine promotes the proliferation of glioma cells and serves as a potential therapeutic target

Zheng Zhu[1,2†], Jiao Wang[1†], Juan Tan[1], Yue-Liang Yao[1], Zhi-Cheng He[1], Xiao-Qing Xie[1], Ze-Xuan Yan[1], Wen-Juan Fu[1], Qing Liu[1], Yan-Xia Wang[1], Tao Luo[1*] and Xiu-Wu Bian[1*]

[1] *Institute of Pathology and Southwest Cancer Center, Southwest Hospital, Third Military Medical University (Army Medical University) and Key Laboratory of Tumor Immunopathology, Ministry of Education of China, Chongqing, PR China*
[2] *Research Department, PLA Rocket Force Characteristic Medical Center, Beijing, PR China*

**Correspondence to: X-W Bian or T Luo, Institute of Pathology and Southwest Cancer Center, Southwest Hospital, Third Military Medical University (Army Medical University) and Key Laboratory of Tumor Immunopathology, Ministry of Education of China, Chongqing 400038, PR China. E-mail: bianxiuwu@263.net (X-W Bian) or lty3169@163.com (T Luo)*

†These authors contributed equally to this work.

Abstract

Calcyphosine (CAPS) was initially identified from the canine thyroid. It also exists in many types of tumor, but its expression and function in glioma remain unknown. Here we explored the clinical significance and the functional mechanisms of CAPS in glioma. We found that CAPS was highly expressed in glioma and high expression of CAPS was correlated with poor survival, in glioma patients and public databases. Cox regression analysis showed that CAPS was an independent prognostic factor for glioma patients. Knockdown of CAPS suppressed the proliferation, whereas overexpression of CAPS promoted the proliferation of glioma both *in vitro* and *in vivo*. CAPS regulated the G2/M phase transition of the cell cycle, but had no obvious effect on apoptosis. CAPS affected PLK1 phosphorylation through interaction with MYPT1. CAPS knockdown decreased p-MYPT1 at S507 and p-PLK1 at S210. Expression of MYPT1 S507 phosphomimic rescued PLK1 phosphorylation and the phenotype caused by CAPS knockdown. The PLK1 inhibitor volasertib enhanced the therapeutic effect of temozolomide in glioma. Our data suggest that CAPS promotes the proliferation of glioma by regulating the cell cycle and the PLK1 inhibitor volasertib might be a chemosensitizer of glioma.

Keywords: CAPS; glioma; proliferation; cell cycle; volasertib

Received 30 January 2021; Revised 26 July 2021; Accepted 5 August 2021

No conflicts of interest were declared.

Introduction

Glioma is the most common tumor in the central nervous system. Glioblastoma (GBM) is the most malignant type of glioma, resulting in a median overall survival of 14–17 months [1]. Rapid proliferation, invasion and drug resistance are important features of GBM [2]. Temozolomide (TMZ) is a DNA-methylating agent used to treat GBM [3,4]. TMZ resistance occurs in some patients and may be one of the reasons for treatment failure [5,6]. Therefore, new targets should be identified for anti-tumor therapy.

Calcyphosine (CAPS) was initially identified in the canine thyroid but has also been detected in humans and other mammals [7–9]. However, CAPS is not expressed in mice or other rodents [10]. CAPS synthesis is increased by thyroid-stimulating hormone and cAMP analogs that promote cell proliferation and maintain cell differentiation [11]. Furthermore, CAPS contains four EF-hand domains for calcium binding [12]. Although the exact function of CAPS is unknown, the characteristics of CAPS suggest that it may participate in both cAMP and calcium-phosphatidylinositol pathways [11]. Recently, CAPS was found to be involved in many kinds of tumor. For example, CAPS is expressed at high levels in ependymoma [13], endometrial cancer [14,15], lung cancer [16], colorectal cancer [17], and esophageal cancer [18]. CAPS may also be a potential predictive marker of tamoxifen resistance in breast cancer [19]. However, the expression and roles of CAPS in glioma remain unknown.

In this study, we used human samples and public databases to analyze the expression and the clinicopathologic relevance of CAPS in glioma. We also investigated the function of CAPS both *in vitro* and *in vivo*. We found that CAPS may be a potential target for anti-glioma therapy.

Materials and methods

Patient samples and public databases

Glioma samples were collected from 172 patients at Southwest Hospital (Chongqing, PR China). All patients underwent surgical excision between 2015 and 2017. Each sample was independently diagnosed by two experienced pathologists. This study was performed according to the principles of the Declaration of Helsinki and approved by the Ethics Committee of Southwest Hospital. The information for glioma samples in the TCGA database was downloaded from http://xena.ucsc.edu/. Data from Rembrandt and GSE16011 databases were downloaded from http://gliovis.bioinfo.cnio.es [20–22].

Antibodies

The following antibodies were used in this study: anti-CAPS antibody (HPA043520, Sigma-Aldrich, St. Louis, MO, USA), anti-GAPDH antibody (5174S, Cell Signaling Technology, Danvers, MA, USA), anti-HA-Tag (C29F4) rabbit antibody (3724S, Cell Signaling Technology), anti-DYKDDDDK Tag (D6W5B) rabbit antibody (14793S, Cell Signaling Technology), Cell Cycle Phase Determination Antibody Sampler Kit (17497T, Cell Signaling Technology), MYPT1 Antibody Sampler Kit (5143T, Cell Signaling Technology), anti-RPS27A antibody (ab172293, Abcam, Cambridge, UK), anti-PLK1 antibody (4513S, Cell Signaling Technology), and anti-p-PLK1 (Thr210) antibody (9062S, Cell Signaling Technology). All primary antibodies were diluted at 1:1,000 for western blotting.

Immunohistochemistry

Formalin-fixed samples were embedded in paraffin wax and sectioned at a thickness of 3 μm. Sections were deparaffinized and rehydrated using a graded series of ethanol solutions. After antigen retrieval and blocking, the sections were incubated overnight with an anti-CAPS antibody (HPA043520, 1:200, Sigma-Aldrich) at 4 °C. After washing, a secondary antibody (K500711-2, Dako, Glostrup, Denmark) was added and incubated for 30 min at 37 °C. All sections were counterstained with hematoxylin. Five random images of each sample were captured, and the integrated optical density (IOD) was measured using Image-Pro Plus 6.0 software (MEDIA Cybernetics, Rockville, MD, USA).

Cells and cell culture

The normal human glial cell line HEB was provided by Dr Guang-Mei Yan (Department of Pharmacology, Sun Yat-Sen University, Guangzhou, PR China; [23–25]). LN229, U87, and 293T cell lines were purchased from the American Type Culture Collection (Manassas, VI, USA). The primary glioma cell lines (GBM1, GBM2, and GBM3) were generated in our laboratory [23]. Cells were cultured in DMEM supplemented with 10% FBS (Gibco; Thermo Fisher Scientific, Waltham, MA, USA) at 37 °C in the presence of 5% CO_2. All cells were tested and found to be negative for mycoplasma and were authenticated by short tandem repeat profiling.

Overexpression and silencing of CAPS

Lentiviral plasmids expressing shRNAs for CAPS, CAPS-Flag, and a negative control were synthesized by Invitrogen (Thermo Fisher Scientific). The sequences of shRNAs are listed in supplementary material, Table S1. ShRNAs and the negative control were inserted into pLKO.1-Puro vectors, whereas Flag-tagged CAPS, HA-tagged MYPT1, and H2B-GFP were inserted into pCDH-CMV-MCS-EF1-Puro vectors. pCDNA3.1 vector expressing MYPT1 S507E was constructed by Hanbio Biotechnology (Shanghai, PR China).

Cell Counting Kit-8 assay

Cells were seeded in 96-well plates at a density of 1,000–2,000 cells per well, with five replicate wells per group. Cell Counting Kit-8 reagent (C0037, Beyotime Biotechnology, Shanghai, PR China) was added to the cells and incubated for 2 h at 37 °C. The color produced was measured using a microplate reader (Thermo Fisher Scientific) at a wavelength of 450 nm. Cell viability was recorded for six continuous days.

5-ethynyl-2'-deoxyuridine assay

A 5-ethynyl-2'-deoxyuridine (EdU) kit (C0071L) was purchased from Beyotime Biotechnology. The EdU assay was carried out according to the manufacturer's protocol. Cells were seeded in 24-well plates at a density of 5,000 cells per well. EdU was added to the culture medium. After 2 h, the cells were washed and fixed with 4% paraformaldehyde for 15 min. Then, the cells were incubated with Click Additive Solution for 30 min. After three washes, the nuclei were stained with DAPI for 10 min. Ten random images of each sample were captured using a confocal microscope (SP5, Leica, Wetzlar, Germany).

Orthotopic transplantation tumor model and drug treatment

Six-week-old NOD-SCID mice (Laboratory Animal Center, Southwest Hospital) were randomly assigned to each group and anesthetized. GBM cells were transduced with luciferase using lentiviruses. GBM cells (2×10^5) were injected into the right frontal lobe. Xenografts were monitored by detecting bioluminescent activity using an *in vivo* imaging system (IVIS, Zeiss, Jena, Germany). The mice in each group received one of the following treatments from the 15th day after tumor implantation: vehicle control (i.p.), volasertib (20 mg/kg, i.p., S2235, Selleck, TX, USA), TMZ (20 mg/kg, i.p., S1237, Selleck), or a combination of volasertib and TMZ. TMZ was only administered for 5 days

(one cycle). Volasertib was administered twice a week for 3 weeks. The mice were sacrificed when neurologic symptoms were apparent and were considered deceased in the survival analysis. Animal experiments were carried out according to the Guide for the Use of Laboratory Animals.

Cell cycle and apoptosis analysis

The cell cycle was analyzed using propidium iodide (PI) staining. Cells were collected and washed with PBS. The cell pellets were fixed overnight with 75% ethanol at 4 °C. The fixed cells were centrifuged at 1,000 × *g* for 5 min and washed two times with cold PBS. Then, the cells were resuspended in an RNase A and PI solution and incubated for 30 min at 37 °C. Cell apoptosis was analyzed using Annexin V/PI double staining. The cells were collected and resuspended in FACS buffer. Annexin V and PI were added to the cell suspension and the cells incubated for 20 min at 4 °C. The cell cycle and apoptosis were analyzed using a flow cytometer (FACSCalibur, BD, Franklin Lakes, NJ, USA).

Reverse transcription-quantitative real-time PCR (RT-qPCR)

Total RNA was extracted using RNAiso (TaKaRa, Otsu, Japan) and was reverse transcribed. SYBR Premix (RR820A, TaKaRa) was used for qPCR performed using a Bio-Rad CFX96 Real-Time PCR Detection System (Bio-Rad, Hercules, CA, USA). The experiment was repeated three times and the results were normalized to GAPDH. The sequences of the primers are listed in supplementary material, Table S2.

Cell synchronization

GBM cells were synchronized at the G1/S boundary by double-thymidine block. First, GBM cells were treated with 2 mM thymidine (Solarbio, Beijing, PR China) for 24 h. Then, the cells were released into thymidine-free medium for 10 h. Cells were treated with 2 mM thymidine again for 14 h after release.

Co-immunoprecipitation (co-IP) and western blot analyses

Co-IP was carried out using a Pierce co-IP kit (26149, Thermo Scientific) according to the manufacturer's protocol; 10 μg of the specific antibody and IgG were used in each co-IP reaction. Proteins were separated through SDS-PAGE gels and transferred onto PVDF membranes (HPA043520, Bio-Rad). After blocking, the membranes were incubated overnight with the primary antibody at 4 °C. After washing with PBST, the membranes were incubated with HRP-conjugated secondary antibodies (Beyotime Biotechnology) for 1 h. Then proteins were visualized using Super Signal West Femto Maximum Sensitivity Substrate (ECL, Thermo Fisher Scientific) and recorded using a ChemiDocXRS system (Bio-Rad).

Liquid chromatography–mass spectroscopy

Proteins from GBM cells were obtained by IP as described above. Liquid chromatography–mass spectroscopy was carried out and the data were analyzed by the Biomedical Analysis and Testing Center of Third Military Medical University (Army Medical University). Detailed methods may be found in previously published papers [26,27].

Expression of MYPT1 S507E

A plasmid expressing a point mutation of MYPT1 (MYPT1 S507E) was purchased from Hanbio Biotechnology (Shanghai, PR China) and was verified by sequencing. Plasmids were transfected into GBM cells using Lipofectamine 3000 transfection reagent (L3000015, Thermo Fisher Scientific) according to the manufacturer's protocol.

Time-lapse imaging

Glioma cells were transduced with the H2B-GFP fusion protein using the lentivirus vector pCDH-CMV-MCS-EF1-Puro, and positive cells were sorted using flow cytometry. Then, the cells were plated in six-well plates and incubated overnight. The plates were incubated in a live cell imaging system (Zeiss) with normal culture conditions. Images were captured every 5 min for 48 h and were processed and analyzed by AxioVision software (Zeiss).

Clonogenic assay

A clonogenic assay was carried out using a previously described method [28]. Colonies were fixed with 4% paraformaldehyde and stained with 0.1% crystal violet (C0121, Beyotime Biotechnology). The colonies were counted using Image-Pro Plus 6.0 software (MEDIA Cybernetics).

Statistical analyses

Student's *t*-test was used to compare data from two different groups. One-way ANOVA was used to compare data from three or more different groups. The optimal cut-off values for CAPS staining were calculated by performing a receiver operator characteristic curve analysis. A chi-squared analysis was carried out to evaluate the relationship between CAPS expression and clinicopathologic features. A log-rank test was used to compare the survival of different groups. The Cox proportional hazard model was used for univariate and multivariate survival analyses. The combination index was calculated by CompuSyn software using the Chou-Talalay method [29]. All experiments were performed at least three times. All analyses were performed with SPSS version 16.0 (IBM, Armonk, NY, USA). $p < 0.05$ was considered to be statistically significant ($^{*}p < 0.05$, $^{**}p < 0.01$, $^{***}p < 0.001$). The data reported in this study are presented as means ± SD.

Results

CAPS is highly expressed in glioma and predicts poor survival

To evaluate the clinical relevance of CAPS expression in glioma, we used immunohistochemistry (IHC) to examine CAPS protein in 172 glioma samples (Figure 1A). The IOD of CAPS staining was calculated and was found to increase from grade II to grade IV in glioma patients (Figure 1B). CAPS expression was significantly correlated with age, grade, *IDH1* status, and 1p/19q codeletion, but not with gender (Table 1). Both univariate and multivariate analyses suggested that CAPS was an independent prognostic factor

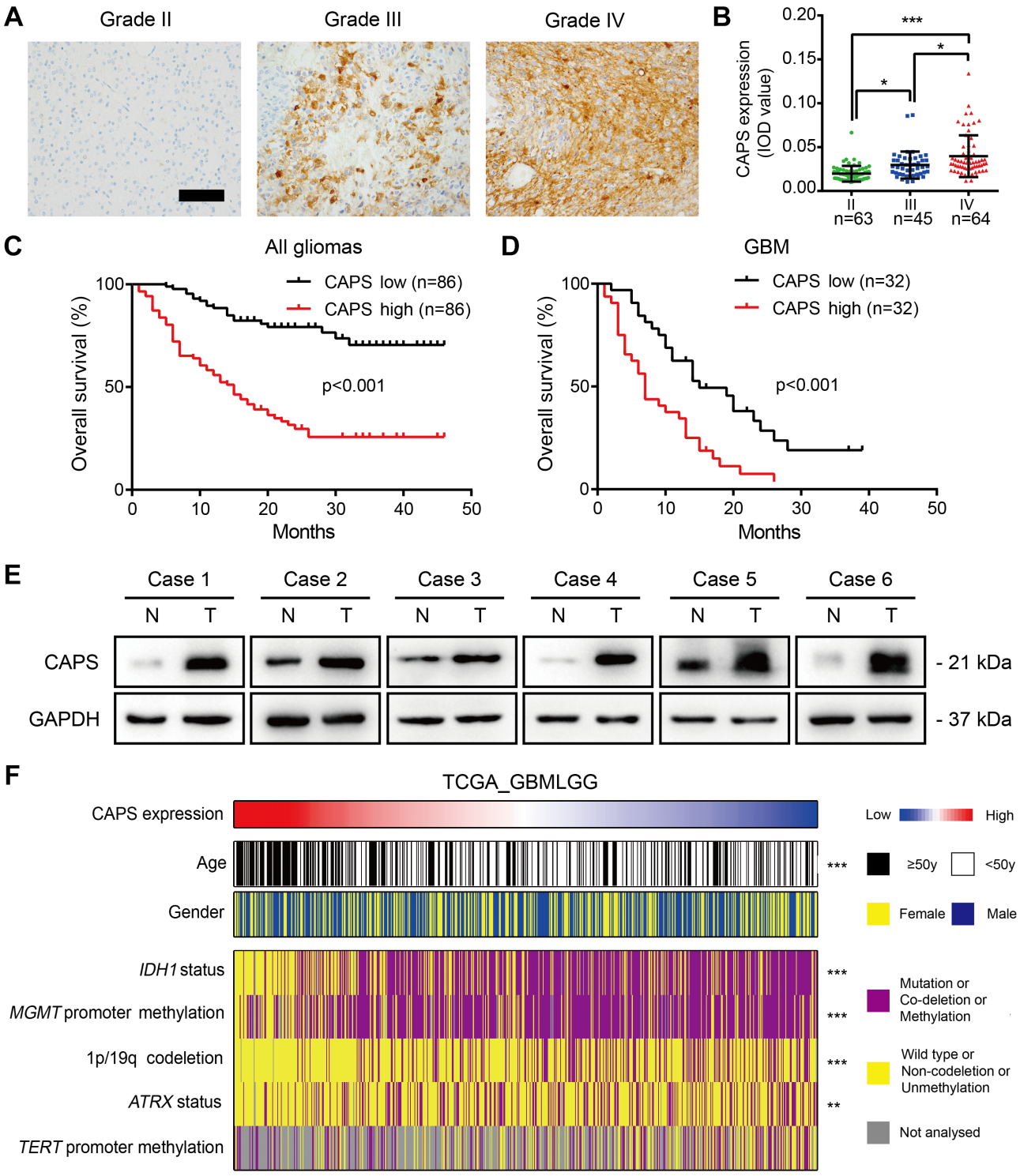

Figure 1. The clinicopathologic relevance of CAPS in glioma. (A) Representative images of CAPS IHC staining in glioma samples. Scale bar = 100 μm. (B) The IOD of CAPS staining in different glioma tissues from patients. (C,D) Survival curves of patients with glioma or GBM presenting high CAPS or low CAPS expression. (E) Analysis of CAPS protein levels in six fresh glioma tissues (diagnosed as GBM, WHO grade IV) (T) paired with adjacent normal tissues (N). (F) Heatmap showing the distribution and association of CAPS expression and clinicopathologic characteristics of patients based on data in the GBM_LGG TCGA database, $n = 667$. One-way ANOVA, $^{*}p < 0.05$, $^{**}p < 0.01$, $^{***}p < 0.001$.

Table 1. The correlation between CAPS expression and clinicopathologic features of glioma patients.

Factors	CAPS low	CAPS high	*P* value
Age (years)			0.005
<50	67 (57.3)	50 (42.7)	
≥50	19 (34.5)	36 (65.5)	
Gender			0.439
Male	48 (47.5)	53 (52.5)	
Female	38 (53.5)	33 (46.5)	
Grade			0.000
II	52 (82.5)	11 (17.5)	
III	19 (42.2)	26 (57.8)	
IV	15 (23.4)	49 (76.5)	
IDH1 status			0.004
Wildtype	46 (41.8)	64 (58.2)	
Mutation	40 (64.5)	22 (35.5)	
1p/19q			0.000
Non-codeletion	58 (43.0)	77 (57.0)	
Codeletion	28 (75.7)	9 (24.3)	

IDH1, isocitrate dehydrogenase 1.

for patients with glioma (Table 2). The survival analyses showed that high CAPS expression was significantly correlated to poor survival of both glioma and GBM patients (Figure 1C,D). We next detected CAPS expression in six freshly resected glioma samples that were diagnosed as GBM and adjacent normal tissues using immunoblot. Data showed that glioma tissues expressed higher level of CAPS than normal tissues (Figure 1E). We further validated *CAPS* expression with information from public databases and found that the mRNA level of *CAPS* in GBM was higher than that in lower grade glioma (LGG) among TCGA, Rembrandt, and GSE16011 datasets (see supplementary material, Figure S1A). High *CAPS* expression was correlated with poor survival of the glioma patients in public databases (see supplementary material, Figure S1B,C). The heatmap shows the relationships between *CAPS* expression and clinicopathologic characteristics obtained from the TCGA database. *CAPS* expression was significantly correlated with age, *IDH1* status, *MGMT* promoter methylation status, 1p/19q codeletion, and *ATRX* status (Figure 1F). These results suggest that CAPS is highly expressed in glioma and is correlated to the poor survival of patients with glioma.

CAPS promotes the proliferation of GBM cells both *in vitro* and *in vivo*

High CAPS expression in glioma indicated that CAPS might play an important role in GBM cells. First, we examined the expression of CAPS in GBM cells. CAPS expression was markedly increased in two GBM cell lines (LN229 and U87) and three primary GBM cell lines (GBM-1, GBM-2, and GBM-3) compared with a normal glial cell line (HEB) (see supplementary material, Figure S2A–C). To investigate the function of CAPS, we used short hairpin RNAs to knockdown CAPS expression and vectors to overexpress CAPS expression in the LN229 and GBM1 cells (see supplementary material, Figure S2D–G). We found that knocking down CAPS significantly suppressed the proliferation of LN229 and GBM1 cells, as measured by the Cell Counting Kit-8 assay (Figure 2A). The percentage of EdU-positive cells was also decreased after CAPS knockdown (Figure 2B,C). By contrast, the overexpression of CAPS promoted the proliferation of GBM cells (see supplementary material, Figure S3A). To verify the function of CAPS *in vivo*, we transduced luciferase into LN229 and GBM1 cells; these cells were then intracranially injected into NOD-SCID mice. Xenografts were detected by *in vivo* bioluminescent imaging (Figure 2D). The results showed that knocking down CAPS significantly suppressed the proliferation of GBM and prolonged the survival of tumor-bearing mice (Figure 2E,F). By contrast, the overexpression of CAPS promoted tumor proliferation and shortened the survival time of tumor-bearing mice (see supplementary material, Figure S3B–D). Taken together, these data suggest that CAPS promotes the proliferation of GBM cells.

CAPS regulates the G2/M transition of GBM cells

To understand how CAPS regulates the proliferation of GBM, we used flow cytometry to analyze the apoptosis of GBM cells. We did not observe a significant difference in the apoptosis rate between the control cells and CAPS-knockdown cells (see supplementary material, Figure S4A,B). Next, we evaluated the cell cycle of the GBM cells and found that knocking down CAPS led to G2/M arrest in the GBM cells (Figure 3A,B). Then, we examined the expression of genes involved in regulating the G2/M phase transition. CCNB1 expression decreased significantly after CAPS knockdown at both the mRNA and protein levels (Figure 3C,D), whereas the levels of other cyclins did not change obviously (see supplementary material, Figure S4C). To confirm the effect of CAPS on cell cycle progression, the GBM cells were synchronized by double thymidine block.

Table 2. Cox regression analysis of prognostic factor analysis for overall survival in glioma patients.

Factors	Univariate Cox regression			Multivariate Cox regression		
	HR	95% CI	*p*	HR	95% CI	*p*
CAPS expression	1.394	1.289–1.504	0.000	1.262	1.144–1.391	0.000
Gender	0.963	0.617–1.504	0.870			
Age	1.033	1.017–1.049	0.000	1.017	1.002–1.031	0.022
Grade	3.351	2.418–4.463	0.000	1.849	1.252–2.732	0.002
Ki67	1.046	1.033–1.059	0.000	1.028	1.011–1.045	0.001
IDH1 status	0.216	0.114–0.408	0.000	0.433	0.219–0.857	0.016
1p19q codeletion	0.177	0.072–0.438	0.000	0.230	0.092–0.576	0.002

CI, confidence interval; HR, hazard ratio; *IDH1*, isocitrate dehydrogenase 1.

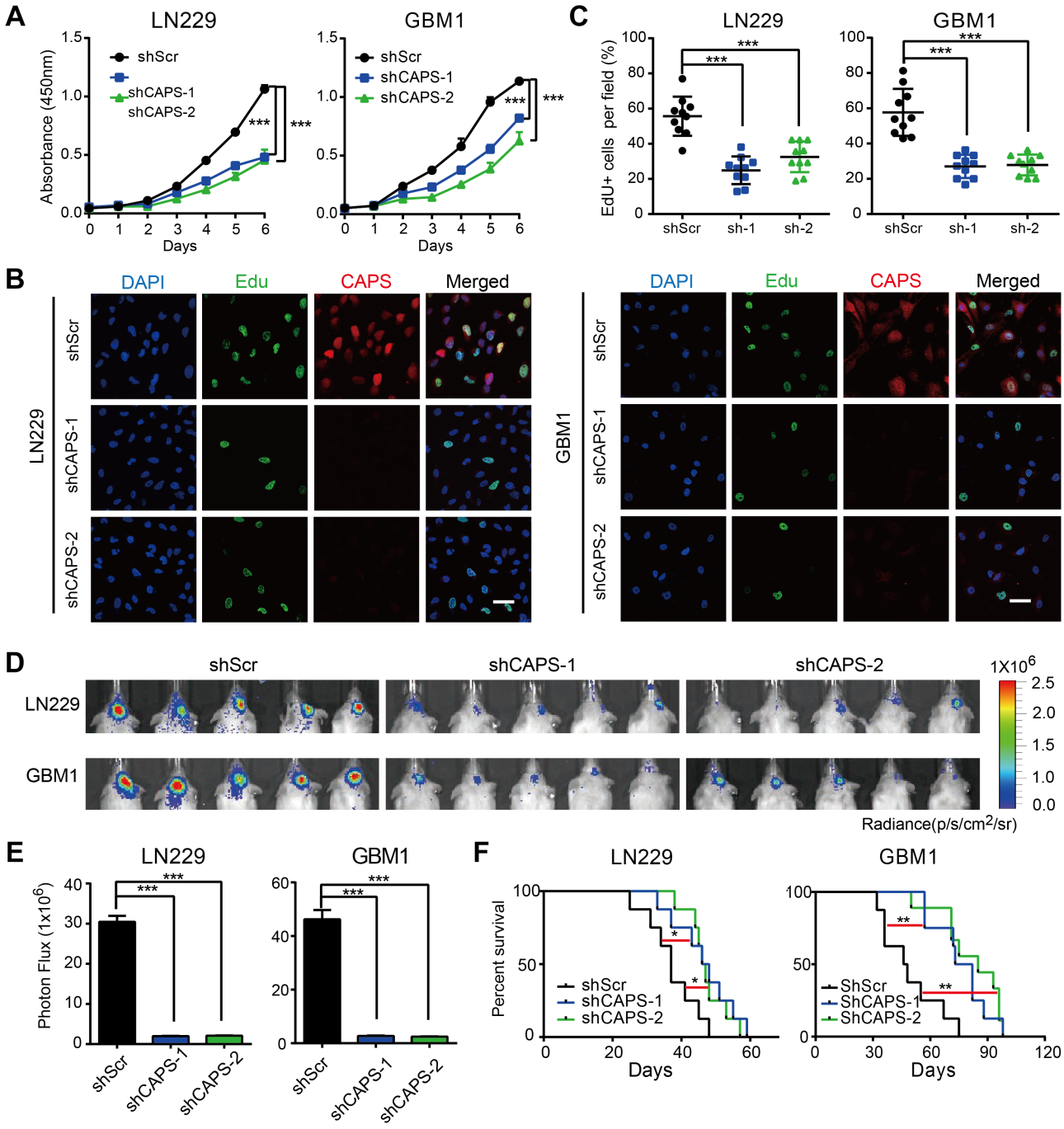

Figure 2. Knockdown of CAPS suppresses the proliferation of GBM cells *in vitro* and *in vivo*. (A) Growth curves of LN229 and GBM1 cells expressing the control shRNA, shCAPS-1, or shCAPS-2. (B) Representative fluorescence images of EdU staining in LN229 and GBM1 cells expressing control shRNA, shCAPS-1, or shCAPS-2. Scale bar = 50 μm. (C) Quantification of the EdU-positive cells shown in (B), $n = 10$. (D,E) Bioluminescence images (D) and quantification (E) of xenografts derived from LN229 and GBM1 cells expressing control shRNA, shCAPS-1, or shCAPS-2. Images were taken on the 21st day. Data are shown as mean ± SD, $n = 5$. (F) Kaplan–Meier survival analysis of mice ($n = 8$) bearing xenografts derived from LN229 and GBM1 cells expressing control shRNA, shCAPS-1, or shCAPS-2. *$p < 0.05$, **$p < 0.01$, ***$p < 0.001$.

Then, the cells were released in fresh medium, and the expression of CCNB1, CCNA2, and CCNE1 was analyzed. The data demonstrated that the cell cycle progression was delayed after CAPS knockdown (Figure 3E). Collectively, these data suggest that CAPS regulates the G2/M phase transition of GBM cells and that CAPS silencing may inhibit tumor proliferation by inducing G2/M phase arrest.

CAPS knockdown delays the mitotic entry of GBM cells

A key event in the G2/M phase is mitosis. To investigate the effects of CAPS on the mitosis phenotypically, we used an H2B-GFP fusion protein to label the nucleus of GBM cells. The mitotic transit times (MTTs) of GBM cells were measured by a live cell imaging system (Figure 4A). The results showed that the average MTTs

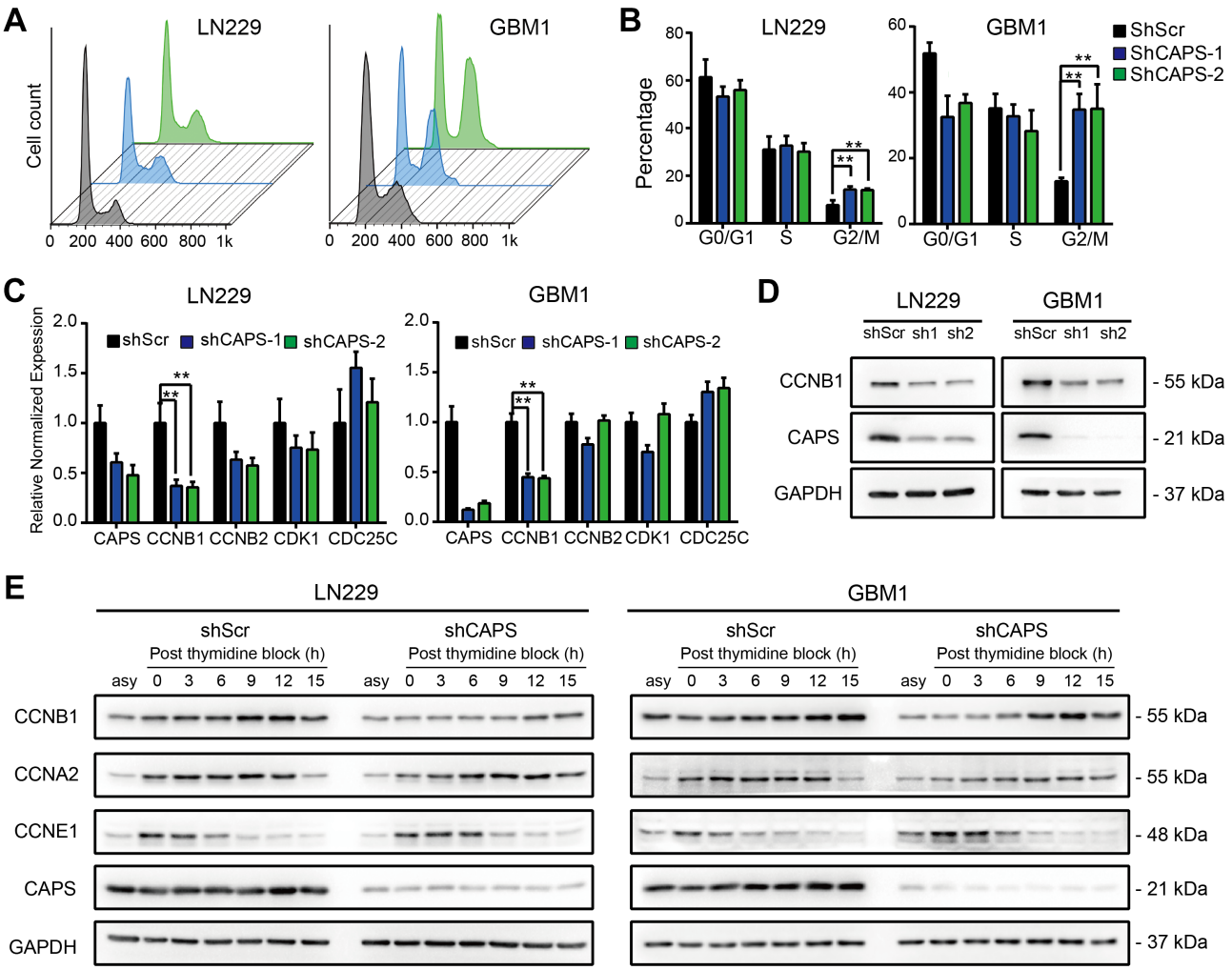

Figure 3. The effects of CAPS on the cell cycle of GBM cells. (A) Cell cycle analysis of LN229 and GBM1 cells expressing control shRNA, shCAPS-1, or shCAPS-2. (B) The quantification of the percentage of cells in the G0/G1, S, and G2/M phases. Data are shown as mean ± SD, $n = 3$. (C) RT-qPCR analysis of genes involved in the G2/M phase transition in LN229 and GBM1 cells expressing control shRNA, shCAPS-1, or shCAPS-2. Data are shown as mean ± SD, $n = 3$. (D) Western blot analysis for the CCNB1 protein in LN229 and GBM1 cells expressing control shRNA, shCAPS-1, or shCAPS-2. (E) LN229 and GBM1 cells were transduced with control shRNA or shCAPS-1. The cells were synchronized through a double thymidine block and collected at different time points after release. The levels of CCNB1, CCNA2, and CCNE1 were analyzed by western blotting. $^{**}p < 0.01$.

in the control cells were 96.0 and 76.7 min in the LN229 and GBM1 cells, respectively. The MTTs increased to 130–150 min as a result of CAPS knockdown (Figure 4B). These results indicate that CAPS regulates mitosis in GBM cells.

CAPS regulates the phosphorylation of PLK1 by interacting with MYPT1

To understand molecular mechanisms of CAPS in GBM, proteins potentially interacting with CAPS in both LN229 and GBM1 cells were obtained by IP and analyzed by mass spectrometry. Twenty-seven proteins were identified in both LN229 and GBM1 cells (Figure 5A and supplementary material, Table S3). We found that two proteins, MYPT1 (also known as PPP1R12A) and RPS27A, were involved in the regulation of the G2/M phase transition (Figure 5A). The co-IP assay confirmed that MYPT1, but not RPS27A, interacted with CAPS in both the LN229 and GBM1 cells (Figure 5B,C). MYPT1 is one of the subunits of myosin phosphatase that can be phosphorylated at different sites during mitosis [30]. We found that knocking down CAPS mainly affected the phosphorylation of S507 in MYPT1 (Figure 5D). PLK1 is a downstream factor of MYPT1 that participates in G2/M phase regulation [31,32]. GBM cells were synchronized and p-PLK1 (T210) levels were detected at different time points after release. The data showed that knocking down CAPS suppressed the phosphorylation of PLK1 at T210 during mitosis (Figure 5E). To explore the connection between CAPS and p-PLK1, we used IHC to examine p-PLK1 protein level in 172 glioma samples. It was found that the expression of p-PLK1 was significantly positively correlated to the expression of CAPS (Figure 5F, supplementary material, Figure S5A). To further analyze the regulatory mechanisms, glutamic acid was substituted for serine at site 507 of MYPT1 to mimic the phosphorylation of S507 in MYPT1. We found that

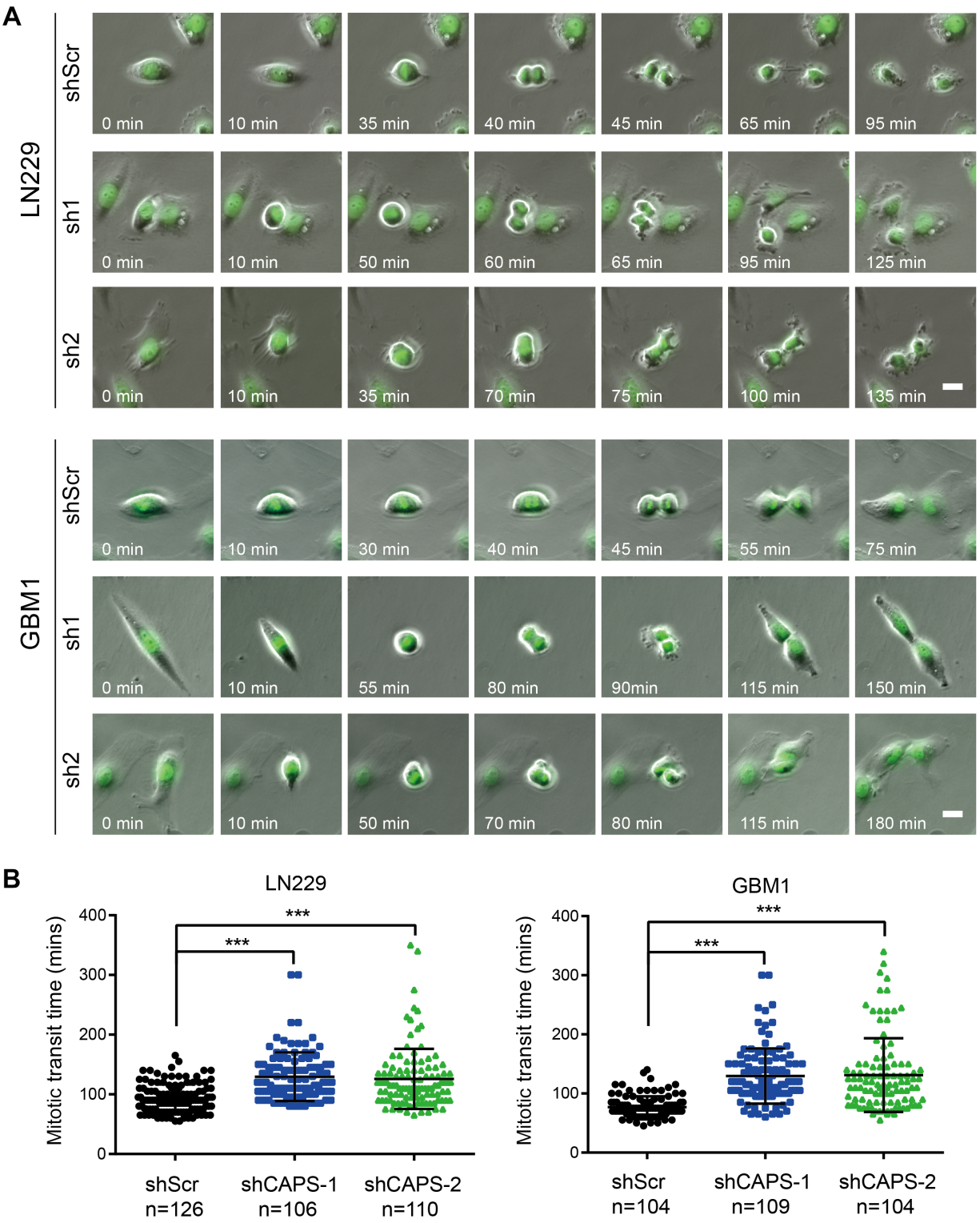

Figure 4. CAPS regulates the mitosis of GBM cells. (A) Representative images obtained with a live cell imaging system. LN229 and GBM1 cells were transduced with H2B-GFP plasmid. GFP-positive cells were sorted and transduced with control shRNA or shCAPS-1. Then, the cells were cultured in a live cell imaging system and photographs were taken every 5 min. Scale bar = 20 μm. (B) Quantification of the MTTs of the GBM cells shown in (A). ***$p < 0.001$.

expression of MYPT1 S507 phosphomimic rescued the PLK1 phosphorylation caused by CAPS knockdown (Figure 5G). We also carried out cell proliferation and cell cycle analyses. The results showed that expression of MYPT1 S507E could partially rescue the inhibition of proliferation and cell cycle arrest induced by CAPS knockdown (Figure 5H,I and supplementary material, Figure S5B). These results suggest that CAPS may regulate the phosphorylation of PLK1 by interacting with MYPT1 in GBM cells.

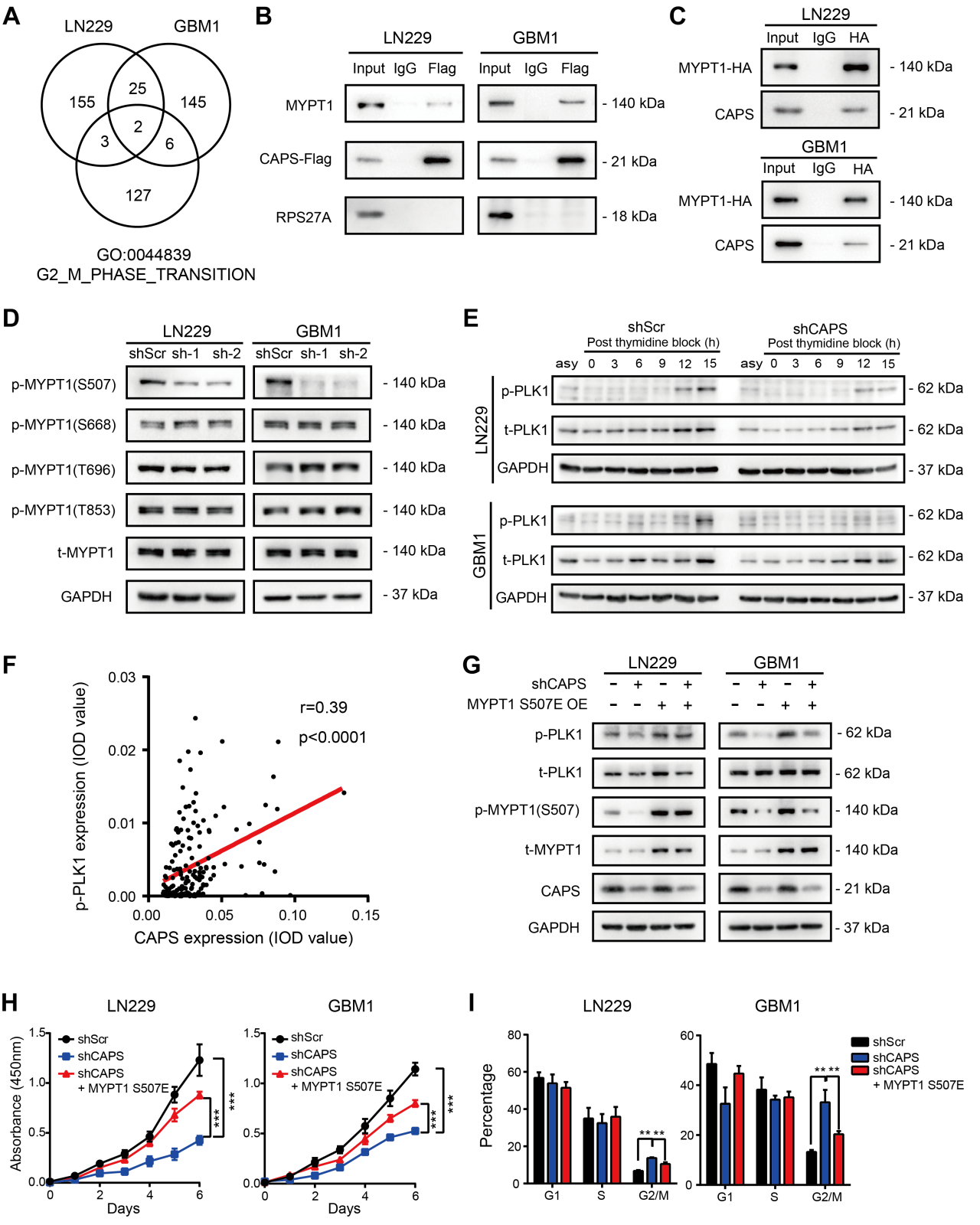

Figure 5. CAPS affects the phosphorylation of PLK1 by interacting with MYPT1. (A) Venn diagram showing 27 genes found to interact with CAPS, among which two genes were involved in the G2/M phase transition. (B,C) Co-IP assay showing the interaction of CAPS with MYPT1, but not with RPS27A. (D) Phosphorylation at different sites of MYPT1 in LN229 and GBM1 cells expressing control shRNA, shCAPS-1, or shCAPS-2, as detected by western blotting. (E) LN229 and GBM1 cells expressing control shRNA or shCAPS-1 were synchronized by a double thymidine block. The levels of p-PLK1 and t-PLK1 were analyzed at different time points after release. (F) Pearson correlation analysis of CAPS and p-PLK1 in 172 glioma samples. (G) Total and phosphorylated PLK1 and MYPT1 were detected by western blotting in LN229 and GBM1 cells expressing control shRNA, shCAPS, or shCAPS+MYPT1 S507E. (H) Proliferation and (I) cell cycle analysis of LN229 and GBM1 cells expressing control shRNA, shCAPS, or shCAPS+MYPT1 S507E. ***$p < 0.001$.

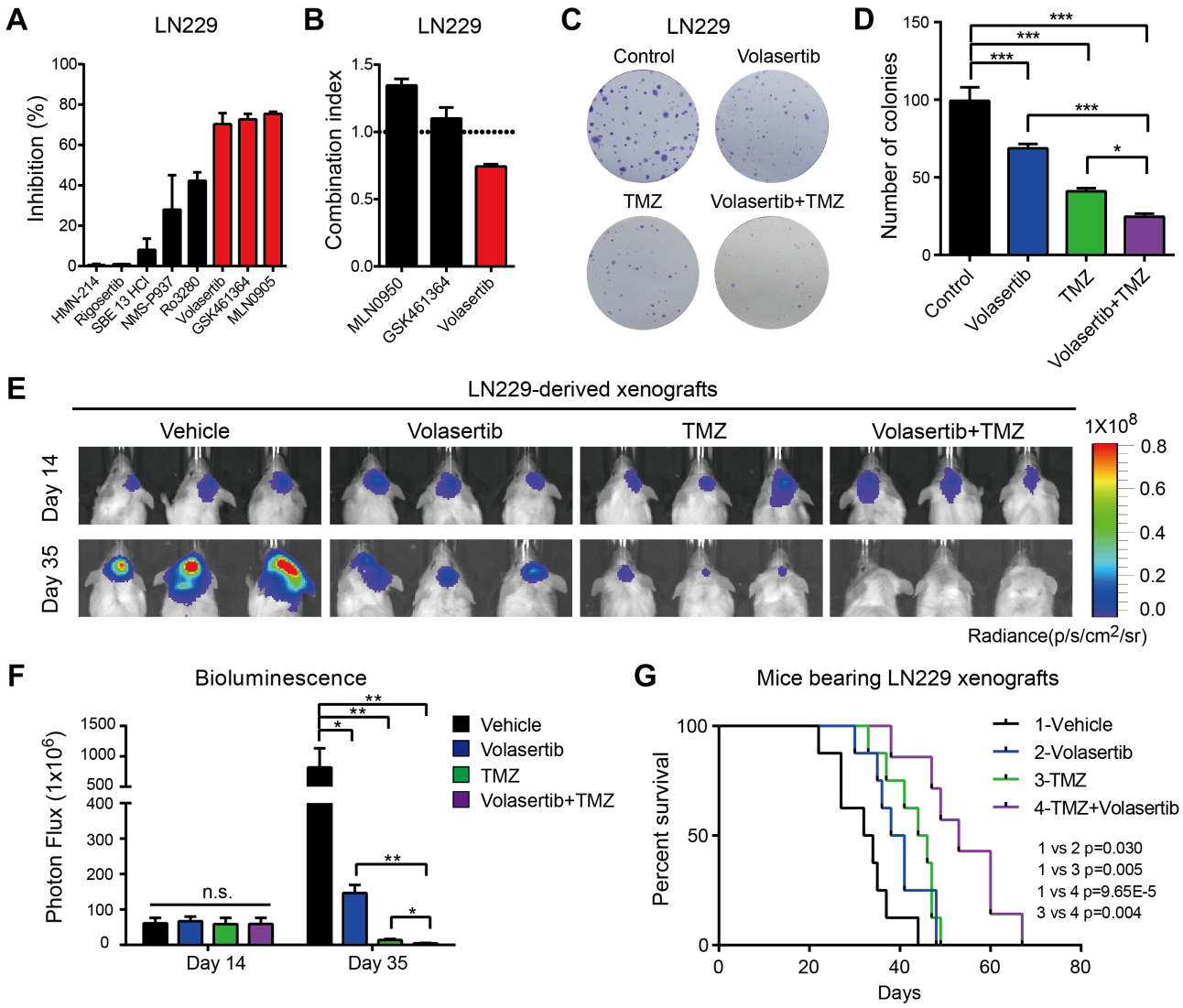

Figure 6. Volasertib enhances the anti-tumor effect of TMZ. (A) Inhibition rate of eight PLK1 inhibitors (20 nM) in LN229 cells. Data are shown as mean ± SD, $n = 3$. (B) The combination indexes of three PLK1 inhibitors and TMZ in LN229 cells. Data are shown as mean ± SD, $n = 3$. (C,D) Colony formation assays using LN229 cells treated with vehicle, volasertib, TMZ, or volasertib in combination with TMZ. Data are shown as mean ± SD, $n = 3$. (E) Bioluminescence images of LN229-derived xenografts in mice before treatment (14 days) and after treatment (35 days). (F) Quantification of the images shown in (E). Data are shown as mean ± SD, $n = 5$. (G) Survival analysis of the mice ($n = 8$) bearing LN229-derived xenografts treated with vehicle, volasertib, TMZ, or volasertib in combination with TMZ. $^*p < 0.05$, $^{**}p < 0.01$, $^{***}p < 0.001$.

Volasertib enhances the anti-glioma effect of TMZ

TMZ is the most common drug used to treat glioma. It causes G2/M arrest of glioma cells by inducing DNA methylation [33]. PLK1 is a downstream molecule of CAPS and an important regulator of the G2/M phase transition. We examined the inhibitory effect of TMZ in control cells and CAPS silencing cells. It was found that CAPS silencing significantly increased the anti-GBM effects of TMZ (see supplementary material, Figure S5C). We hypothesized that the inhibition of PLK1 would be an effective treatment for glioma. Thus, we evaluated the cytotoxicity of eight PLK1 inhibitors and observed that three inhibitors effectively suppressed the proliferation of LN229 cells (Figure 6A) as the three inhibitors had similar IC50 values (see supplementary material, Figure S6A–D). The combination indexes of these three inhibitors and TMZ were calculated using the Chou-Talalay method [29], and only volasertib and TMZ were found to exert a synergistic effect (Figure 6B). A colony formation assay also showed that volasertib had a chemosensitizing effect on TMZ (Figure 6C,D). To confirm the combination effect of TMZ and volasertib *in vivo*, we performed studies using an orthotropic transplant glioma model. After tumorigenesis, the mice without significantly different tumor sizes were randomly assigned to four groups and received different treatments (Figure 6E). Consequently, we observed that volasertib treatment in combination with TMZ significantly decreased tumor size and increased survival time compared with TMZ alone (Figure 6E–G). Taken together, these data indicate that volasertib, a PLK1 inhibitor, in combination with TMZ enhances the therapeutic efficacy.

Discussion

CAPS has been reported to be expressed in many kinds of tumor [14–19], but its role in glioma remains unclear. In the present study, by analyzing our glioma patients' data and public databases, we found that CAPS was upregulated in GBM compared with LGG. High CAPS expression was correlated to poor survival of patents with glioma. Inter- and intratumoral heterogeneity limited the application of bulk tumor gene expression profiling. Therefore, we used our patient sample and three public databases to make the results more credible. Rapid proliferation contributes to the malignancy of GBM [2]. Our results showed that CAPS knockdown significantly suppressed the proliferation of LN229 and GBM1 cells (Figure 2A–C). The efficiency of inhibition was slightly different in the two cell lines. This result reflected the intertumoral heterogeneity of GBM. Our data also showed that CAPS promoted GBM cell proliferation by regulating the cell cycle. These results indicate that CAPS plays an oncogenic role in glioma.

Previous studies reported that CAPS was involved in both calcium-phosphatidylinositol and cAMP signaling cascades in the canine thyroid [11]. However, the mechanisms by which CAPS regulates the biologic features of tumors remain unclear. Notably, our study revealed an interaction between CAPS and MYPT1. MYPT1 is one of five mammalian MYPT family genes [30]. It is a key regulator of protein phosphatase 1C and plays important roles in smooth muscle contraction, development, and the cell cycle [34–38]. The binding of PLK1 to the MYPT1-PP1c complex dephosphorylates T210 in PLK1 [31]. Our data indicated that knockdown of CAPS might attenuate the phosphorylation of MYPT1 at S507. Subsequently, the activity of PLK1, a key regulator of the G2/M phase transition, was reduced. Furthermore, expression of MYPT1 S507 phosphomimic rescued PLK1 phosphorylation and the phenotype caused by CAPS knockdown. These results further elucidate the mechanism of CAPS in regulating mitosis.

Based on our findings, strategies targeting CAPS may block the cell cycle and exert a therapeutic effect on GBM. Inhibitors of CAPS are not available; therefore, we searched for downstream CAPS-regulated targets. Volasertib, a selective inhibitor of PLK1, markedly suppressed the proliferation of GBM cells and exerted a synergistic effect with TMZ. Using an orthotropic xenograft model, we found that volasertib treatment in combination with TMZ significantly inhibited GBM proliferation and increased the survival of tumor-bearing mice. These results are consistent with previous studies [39–43]. We noticed that the prolongation of survival time was not as obvious as the reduction of tumor volume. These findings may be related to the intraheterogeneity of tumor and tumor stem cells [44–46]. Volasertib has emerged successfully from phase 2 trials with acceptable side-effects and has entered a phase 3 trial (NCT01721876) for the treatment of acute myeloid leukemia [47]. In the present study, we expanded the potential application of volasertib as a treatment for GBM in combination with TMZ. However, tumor heterogeneity is indeed an important challenge for targeted therapy. It is important to find suitable biomarkers to identify the patients who can benefit from cell cycle kinase inhibitor treatment with fewer side-effects. Further investigations are required to determine whether volasertib is suitable for clinical use.

In summary, our data demonstrate that high expression of CAPS promotes the proliferation of GBM cells and results in poor survival of patients with GBM. CAPS regulates G2/M phase transition of GBM cells through interaction with MYPT1. Our preclinical studies provide evidence for the use of volasertib as a treatment for GBM.

Acknowledgements

We thank Qinghua Ma, Ruili Cai, and Jingya Miao from the Institute of Pathology and Southwest Cancer Center, Southwest Hospital for their help with flow cytometry.

Author contributions statement

All authors contributed significantly to the content of the manuscript. TL, ZZ, JW, ZH and WF collected samples and performed IHC staining. ZZ, JW, JT, YY, XX, ZY and QL performed *in vitro* experiments. ZZ, XX, ZY and YW performed *in vivo* experiments. ZZ and TL analyzed and interpreted data. XB revised the manuscript. All authors were involved in writing the paper and approved the final manuscript.

References

1. Molinaro AM, Taylor JW, Wiencke JK, *et al*. Genetic and molecular epidemiology of adult diffuse glioma. *Nat Rev Neurol* 2019; **15:** 405–417.
2. Aldape K, Zadeh G, Mansouri S, *et al*. Glioblastoma: pathology, molecular mechanisms and markers. *Acta Neuropathol* 2015; **129:** 829–848.
3. Minniti G, De Sanctis V, Muni R, *et al*. Radiotherapy plus concomitant and adjuvant temozolomide for glioblastoma in elderly patients. *J Neurooncol* 2008; **88:** 97–103.
4. Stupp R, Mason WP, van den Bent MJ, *et al*. Radiotherapy plus concomitant and adjuvant temozolomide for glioblastoma. *N Engl J Med* 2005; **352:** 987–996.
5. Stavrovskaya AA, Shushanov SS, Rybalkina EY. Problems of glioblastoma multiforme drug resistance. *Biochemistry (Mosc)* 2016; **81:** 91–100.
6. Lee SY. Temozolomide resistance in glioblastoma multiforme. *Genes Dis* 2016; **3:** 198–210.
7. Lecocq R, Lamy F, Dumont JE. Pattern of protein phosphorylation in intact stimulated cells: thyrotropin and dog thyroid. *Eur J Biochem* 1979; **102:** 147–152.

8. El Housni H, Radulescu A, Lecocq R, *et al*. Cloning and sequence analysis of human calcyphosine complementary DNA. *Biochim Biophys Acta* 1997; **1352:** 249–252.
9. Cuneo KC, Vredenburgh JJ, Sampson JH, *et al*. Safety and efficacy of stereotactic radiosurgery and adjuvant bevacizumab in patients with recurrent malignant gliomas. *Int J Radiat Oncol Biol Phys* 2012; **82:** 2018–2024.
10. Clément S, Dumont JE, Schurmans S. Loss of calcyphosine gene expression in mouse and other rodents. *Biochem Biophys Res Commun* 1997; **232:** 407–413.
11. Lefort A, Lecocq R, Libert F, *et al*. Cloning and sequencing of a calcium-binding protein regulated by cyclic AMP in the thyroid. *EMBO J* 1989; **8:** 111–116.
12. Dong H, Li X, Lou Z, *et al*. Crystal-structure and biochemical characterization of recombinant human calcyphosine delineates a novel EF-hand-containing protein family. *J Mol Biol* 2008; **383:** 455–464.
13. de Bont JM, den Boer ML, Kros JM, *et al*. Identification of novel biomarkers in pediatric primitive neuroectodermal tumors and ependymomas by proteome-wide analysis. *J Neuropathol Exp Neurol* 2007; **66:** 505–516.
14. Li Z, Min W, Huang C, *et al*. Proteomics-based approach identified differentially expressed proteins with potential roles in endometrial carcinoma. *Int J Gynecol Cancer* 2010; **20:** 9–15.
15. Li Z, Huang C, Bai S, *et al*. Prognostic evaluation of epidermal fatty acid-binding protein and calcyphosine, two proteins implicated in endometrial cancer using a proteomic approach. *Int J Cancer* 2008; **123:** 2377–2383.
16. Pastor MD, Nogal A, Molina-Pinelo S, *et al*. Identification of proteomic signatures associated with lung cancer and COPD. *J Proteomics* 2013; **89:** 227–237.
17. Shao W, Wang Q, Wang F, *et al*. Abnormal expression of calcyphosine is associated with poor prognosis and cell biology function in colorectal cancer. *Onco Targets Ther* 2016; **9:** 477–487.
18. Li F, Zhu D, Yang Y, *et al*. Overexpression of calcyphosine is associated with poor prognosis in esophageal squamous cell carcinoma. *Oncol Lett* 2017; **14:** 6231–6237.
19. Johansson HJ, Sanchez BC, Forshed J, *et al*. Proteomics profiling identify CAPS as a potential predictive marker of tamoxifen resistance in estrogen receptor positive breast cancer. *Clin Proteomics* 2015; **12:** 8.
20. Madhavan S, Zenklusen JC, Kotliarov Y, *et al*. Rembrandt: helping personalized medicine become a reality through integrative translational research. *Mol Cancer Res* 2009; **7:** 157–167.
21. Gravendeel LA, Kouwenhoven MC, Gevaert O, *et al*. Intrinsic gene expression profiles of gliomas are a better predictor of survival than histology. *Cancer Res* 2009; **69:** 9065–9072.
22. Bowman RL, Wang Q, Carro A, *et al*. GlioVis data portal for visualization and analysis of brain tumor expression datasets. *Neuro Oncol* 2017; **19:** 139–141.
23. Shi Y, Chen C, Zhang X, *et al*. Primate-specific miR-663 functions as a tumor suppressor by targeting PIK3CD and predicts the prognosis of human glioblastoma. *Clin Cancer Res* 2014; **20:** 1803–1813.
24. Wu S, Lin Y, Xu D, *et al*. MiR-135a functions as a selective killer of malignant glioma. *Oncogene* 2012; **31:** 3866–3874.
25. Kumar B, Hovland AR, Prasad JE, *et al*. Establishment of human embryonic brain cell lines. *In Vitro Cell Dev Biol Anim* 2001; **37:** 259–262.
26. Willenberg I, Ostermann AI, Schebb NH. Targeted metabolomics of the arachidonic acid cascade: current state and challenges of LC-MS analysis of oxylipins. *Anal Bioanal Chem* 2015; **407:** 2675–2683.
27. Ma Q, Liang M, Wu Y, *et al*. Osteoclast-derived apoptotic bodies couple bone resorption and formation in bone remodeling. *Bone Res* 2021; **9:** 5.
28. Franken NA, Rodermond HM, Stap J, *et al*. Clonogenic assay of cells in vitro. *Nat Protoc* 2006; **1:** 2315–2319.
29. Chou TC. Drug combination studies and their synergy quantification using the Chou-Talalay method. *Cancer Res* 2010; **70:** 440–446.
30. Grassie ME, Moffat LD, Walsh MP, *et al*. The myosin phosphatase targeting protein (MYPT) family: a regulated mechanism for achieving substrate specificity of the catalytic subunit of protein phosphatase type 1delta. *Arch Biochem Biophys* 2011; **510:** 147–159.
31. Yamashiro S, Yamakita Y, Totsukawa G, *et al*. Myosin phosphatase-targeting subunit 1 regulates mitosis by antagonizing polo-like kinase 1. *Dev Cell* 2008; **14:** 787–797.
32. Archambault V, Glover DM. Polo-like kinases: conservation and divergence in their functions and regulation. *Nat Rev Mol Cell Biol* 2009; **10:** 265–275.
33. Friedman HS, Kerby T, Calvert H. Temozolomide and treatment of malignant glioma. *Clin Cancer Res* 2000; **6:** 2585–2597.
34. Geeves MA, Holmes KC. Structural mechanism of muscle contraction. *Annu Rev Biochem* 1999; **68:** 687–728.
35. Okamoto R, Ito M, Suzuki N, *et al*. The targeted disruption of the MYPT1 gene results in embryonic lethality. *Transgenic Res* 2005; **14:** 337–340.
36. Weiser DC, Row RH, Kimelman D. Rho-regulated myosin phosphatase establishes the level of protrusive activity required for cell movements during zebrafish gastrulation. *Development* 2009; **136:** 2375–2384.
37. Chiyoda T, Sugiyama N, Shimizu T, *et al*. LATS1/WARTS phosphorylates MYPT1 to counteract PLK1 and regulate mammalian mitotic progression. *J Cell Biol* 2012; **197:** 625–641.
38. Toledo CM, Ding Y, Hoellerbauer P, *et al*. Genome-wide CRISPR-Cas9 screens reveal loss of redundancy between PKMYT1 and WEE1 in glioblastoma stem-like cells. *Cell Rep* 2015; **13:** 2425–2439.
39. Pezuk JA, Brassesco MS, Morales AG, *et al*. Polo-like kinase 1 inhibition causes decreased proliferation by cell cycle arrest, leading to cell death in glioblastoma. *Cancer Gene Ther* 2013; **20:** 499–506.
40. Amani V, Prince EW, Alimova I, *et al*. Polo-like kinase 1 as a potential therapeutic target in diffuse intrinsic pontine glioma. *BMC Cancer* 2016; **16:** 647.
41. Higuchi F, Fink AL, Kiyokawa J, *et al*. PLK1 inhibition targets Myc-activated malignant glioma cells irrespective of mismatch repair deficiency-mediated acquired resistance to temozolomide. *Mol Cancer Ther* 2018; **17:** 2551–2563.
42. Koncar RF, Chu Z, Romick-Rosendale LE, *et al*. PLK1 inhibition enhances temozolomide efficacy in IDH1 mutant gliomas. *Oncotarget* 2017; **8:** 15827–15837.
43. Liu N, Hu G, Wang H, *et al*. PLK1 inhibitor facilitates the suppressing effect of temozolomide on human brain glioma stem cells. *J Cell Mol Med* 2018; **22:** 5300–5310.
44. Nicholson JG, Fine HA. Diffuse glioma heterogeneity and its therapeutic implications. *Cancer Discov* 2021; **11:** 575–590.
45. Suvà ML, Tirosh I. The glioma stem cell model in the era of single-cell genomics. *Cancer Cell* 2020; **37:** 630–636.
46. Patel AP, Tirosh I, Trombetta JJ, *et al*. Single-cell RNA-seq highlights intratumoral heterogeneity in primary glioblastoma. *Science* 2014; **344:** 1396–1401.
47. Döhner H, Lübbert M, Fiedler W, *et al*. Randomized, phase 2 trial of low-dose cytarabine with or without volasertib in AML patients not suitable for induction therapy. *Blood* 2014; **124:** 1426–1433.

SUPPLEMENTARY MATERIAL ONLINE

Figure S1. Analysis of *CAPS* expression in public databases

Figure S2. Expression of CAPS in glioma cells

Figure S3. Overexpression of CAPS promotes the proliferation of GBM cells

Figure S4. Knockdown of CAPS does not significantly increase apoptosis in GBM cells

Figure S5. CAPS regulates the phosphorylation of PLK1

Figure S6. IC50 of TMZ and three PLK1 inhibitors

Table S1. Sequences of shRNAs used in this study

Table S2. Primers used for qPCR

Table S3. Proteins potentially interacting with CAPS in GBM cells